IOPscience iopscience.iop.org

Home Search Collections Journals About Contact us My IOPscience

Fluctuations in quantum expectation values for chaotic systems with broken time-reversal symmetry

This article has been downloaded from IOPscience. Please scroll down to see the full text article.

1998 J. Phys. A: Math. Gen. 31 5631

(http://iopscience.iop.org/0305-4470/31/26/004)

View the table of contents for this issue, or go to the journal homepage for more

Download details:
IP Address: 171.66.16.122
The article was downloaded on 02/06/2010 at 06:56

Please note that terms and conditions apply.

J. Phys. A: Math. Gen. **31** (1998) 5631–5640. Printed in the UK PII: S0305-4470(98)92291-0

Fluctuations in quantum expectation values for chaotic systems with broken time-reversal symmetry

T O de Carvalho†§, J P Keating†‡ and J M Robbins†‡

† School of Mathematics, University Walk, Bristol BS8 1TW, UK

‡ Basic Research Institute in the Mathematical Sciences, Hewlett-Packard Laboratories, Filton Road, Stoke Gifford, Bristol BS12 6QZ, UK

Received 6 March 1998

Abstract. The semiclassical analysis of Eckhardt *et al* for the variance of quantum expectation values in classically chaotic systems is extended to obtain the transitional form as time-reversal symmetry is gradually broken. Numerical results for a family of perturbed cat maps confirm this analysis, including the halving of the variance as time-reversal symmetry is fully broken.

1. Introduction

We study the approach to the classical limit of the diagonal matrix elements of an operator A, assumed to correspond to a classical observable $A_c(z)$, in the eigenstate basis of a classically chaotic quantum system. The quantum equidistribution theorem of Shnirelman [1], further developed by Zelditch [2] and Colin de Verdiére [3], states that, for classically ergodic systems, the diagonal elements A_n tend to the microcanonical average of $A_c(z)$.

Eckhardt *et al* [4] developed a semiclassical theory for the variance σ^2 of the expectation values A_n, thereby establishing the rate at which the classical limit is approached. For strongly chaotic systems (for example, systems for which correlation functions decay faster than $1/t$), they obtained the result

$$\sigma^2 = \frac{\alpha}{T_H} g \tag{1}$$

where $\alpha = \langle A_c^2 \rangle_E$ is related to the classical variance ($\langle \cdot \rangle_E$ denotes the average over the energy shell), T_H is the Heisenberg time (i.e. the time conjugate to the mean level separation) of the system, and g is a symmetry factor equal to 2 for time-reversal invariant systems and 1 for systems without time-reversal symmetry.

Time reversal is a symmetry linked to a global property of the spectrum. In random matrix theory, systems without time-reversal symmetry belong to the unitary ensemble (the Gaussian unitary ensemble (GUE) for Hamiltonians; the circular unitary ensemble (CUE) for unitary operators), whereas time-reversal invariant systems (without spin) belong to the orthogonal ensemble (the Gaussian orothogonal ensemble (GOE) and the circular orthogonal ensemble (COE), respectively). A central theme of quantum chaology is the conjecture [5, 6], supported by extensive numerical evidence [7] and semiclassical theories [8–11], that this classification also applies to classically chaotic quantum systems in the semiclassical limit.

§ Present address: Departamento de Matemática, ICEx—UFMG, CP 702, Belo Horizonte, 30161-970, Brazil.

0305-4470/98/265631+10$19.50 © 1998 IOP Publishing Ltd

Much attention has been paid to the transition between the orthogonal and unitary ensembles [12, 13]. Our purpose here is to study the variance of diagonal matrix elements in this regime, both in terms of a semiclassical theory based on the trace formula and direct numerical calculations. The results obtained also hold for systems with false broken time-reversal symmetry [14, 15].

This paper is organized as follows. In section 2, we obtain the transitional behaviour of the variance σ^2 as time-reversal symmetry is gradually broken. The result is of the form (1), but the factor g is found to depend on a symmetry-breaking parameter, decreasing from 2 to 1 as this parameter increases. We compare this expression with numerical calculations of quantum expectation values for a family of strongly chaotic systems (section 4). The systems we consider, perturbed cat maps, are described briefly in section 3.

2. Derivation of the variance

We consider quantum maps, although essentially the same analysis can be applied to quantum Hamiltonians. A quantum map is represented by a unitary matrix U, whose dimension N plays the role of the inverse of Planck's constant. We denote its eigenvectors and eigenvalues by $|n\rangle$ and $\exp(-\mathrm{i}\theta_n)$. U corresponds to a classical map ϕ, assumed to be chaotic. Let A be a quantum observable with classical limit $A_c(z)$. For convenience we take A to be traceless, so that its diagonal matrix elements $A_n = \langle n|A|n\rangle$ have zero mean, and the phase-space average of $A_c(z)$ vanishes. Let

$$\sigma^2 = \frac{1}{N}\sum_{n=1}^{N} A_n^2 \tag{2}$$

denote the variance of the A_n.

Our analysis is a straightforward extension of that of Eckhardt *et al* [4], who obtained a semiclassical expression for σ^2 for systems with and without time-reversal symmetry. Here we allow the dynamics to depend on a parameter κ which gradually breaks time-reversal symmetry, or more generally, an anticanonical symmetry. An anticanonical symmetry K is an involution (i.e. $K \circ K = 1$) obtained from the composition of the time-reversal map T with a canonical transformation; a classical map ϕ is invariant under K if $K \circ \phi \circ K = \phi^{-1}$. For ease of discussion, we shall, in this section, take K to be simply time reversal itself (although for the family of maps considered in section 3, this will not be the case). Thus, we suppose ϕ has time-reversal symmetry only for $\kappa = 0$. A is assumed to be κ-independent and time-reversal invariant (i.e. $A_c \circ T = A_c$). To make the discussion self-contained, we present the derivation in full.

Consider the smoothed, weighted spectral density,

$$\begin{aligned} d_A(\theta) &= \frac{1}{2\pi}\sum_{\tau=-\infty}^{\infty} \mathrm{Tr}(AU^\tau)\mathrm{e}^{\mathrm{i}\tau\theta} h_\epsilon(|\tau|) \\ &= \sum_{n=1}^{N} A_n \delta_\epsilon(\theta - \theta_n). \end{aligned} \tag{3}$$

Here $h_\epsilon(|\tau|)$ is a smooth cut-off function, decreasing from 1, when $|\tau| \ll 1/\epsilon$, to 0, when $|\tau| \gg 1/\epsilon$. Its discrete Fourier transform,

$$\delta_\epsilon(\theta) = \frac{1}{2\pi}\sum_{\tau=-\infty}^{\infty} \exp(\mathrm{i}\tau\theta) h(|\tau|) \tag{4}$$

is a smoothed periodic delta function with peaks of width ϵ.

Squaring the expression in (3), we obtain

$$d_A^2(\theta) = \sum_{m,n=1}^{N} A_m A_n \delta_\epsilon(\theta - \theta_m)\delta_\epsilon(\theta - \theta_n). \tag{5}$$

Taking ϵ to be smaller than the mean eigenangle spacing ($= 2\pi/N$), we may neglect the off-diagonal ($m \neq n$) terms in the sum. For the diagonal terms, we make use of Berry's observation [9] that the product of two δ_ϵ's is again delta-function-like. In particular,

$$\delta_\epsilon^2(\theta - \theta_n) \approx \frac{1}{a\epsilon}\delta_{\epsilon'}(\theta - \theta_n) \tag{6}$$

where the scaled width ϵ' and normalization constant a depend on the particular form of $\delta_\epsilon(\theta)$. Our results do not depend essentially on the chosen form; we note that a is given by

$$\frac{1}{a} = \epsilon \int_0^{2\pi} \delta_\epsilon^2(\theta)\,\mathrm{d}\theta = \frac{\epsilon}{2\pi} \sum_{\tau=-\infty}^{\infty} h_\epsilon^2(|\tau|). \tag{7}$$

Thus, integration of (5) over θ yields the formula

$$\sigma^2 = \frac{a\epsilon}{N} \int_0^{2\pi} d_A^2(\theta)\,\mathrm{d}\theta \tag{8}$$

for the variance.

A semiclassical expression is obtained from the weighted trace formula [16]

$$d_A(\theta) = \frac{1}{2\pi} \sum_p A_p w_p \mathrm{e}^{\mathrm{i}\tau_p\theta + 2\pi\mathrm{i}NS_p} h_\epsilon(|\tau_p|). \tag{9}$$

The sum is taken over periodic orbits p of the classical map, including both positive and negative traversals, with integer periods τ_p, actions S_p and amplitudes $w_p = 1/r_p|\det(M_p - I)|^{-1/2}$ expressed in terms of the monodromy matrix M_p and repetition number r_p. The quantity $A_p = \sum_{s=1}^{\tau_p} A_c(z_s)$ is the classical observable $A_c(z)$ summed along the (not necessarily primitive) orbit.

Squaring the expression in (9), we obtain

$$d_A^2(\theta) = \frac{1}{4\pi^2} \sum_{p,q} A_p A_q w_p w_q \mathrm{e}^{\mathrm{i}(\tau_p - \tau_q)\theta + 2\pi\mathrm{i}N(S_p - S_q)} h_\epsilon(|\tau_p|) h_\epsilon(|\tau_q|). \tag{10}$$

We evaluate the double sum in the diagonal approximation, which in this case means keeping contributions only from $q = p$ and $q = p^*$, where p^* labels the time reverse of the orbit p when $\kappa = 0$. This is justified by the fact that the off-diagonal contributions are semiclassically smaller [10].

As discussed by Berry and Robnik [17] in the context of Aharonov–Bohm billiards, when $\kappa \neq 0$, the phase differences $\Delta_p = S_p - S_{p^*}$ cause the $q = p^*$ contributions to cancel. Complete cancellation occurs as κ increases over a classically small range, and the differences $A_p - A_{p^*}$ and $w_p - w_{p^*}$ can be neglected for κ in this range. Restricting the orbit sum to positive traversals, we thereby obtain

$$d_A^2(\theta) = \frac{1}{2\pi^2} \sum_p A_p^2 w_p^2 (1 + \mathrm{e}^{2\pi\mathrm{i}N\Delta_p}) h_\epsilon^2(\tau_p). \tag{11}$$

Next, terms in the sum are replaced by their average values for long orbits. Assuming such orbits to be uniformly distributed in phase space, we take A_p to be randomly distributed with zero mean and variance

$$\langle A_p^2 \rangle = \alpha\tau_p \tag{12}$$

where α is the phase-space average of $A_c^2(z)$. For the phase differences $\Delta_p = S_p - S_{p^*}$, we make the ansatz that these are normally distributed with zero mean and variance $\langle \Delta_p^2 \rangle = \xi \tau_p$ proportional to the period. Averaging the phase factors $\exp(2\pi \mathrm{i} N \Delta_p)$ with respect to this distribution, we find that

$$\langle \mathrm{e}^{2\pi \mathrm{i} N \Delta_p} \rangle = \mathrm{e}^{-2\pi^2 N^2 \xi \tau_p}. \tag{13}$$

As discussed in the appendix (see also [13]), the parameter ξ is proportional to κ^2, and may be estimated empirically from the classical dynamics.

Finally, we invoke the Hannay–Ozorio de Almeida sum rule [8] to replace the weighted sum over orbits $\sum_p \tau_p |w_p|^2$ by a sum over periods $\sum_{\tau=1}^{\infty}$. From these considerations we obtain

$$d^2(\theta) = \frac{\alpha}{2\pi^2} \sum_{\tau=1}^{\infty} (1 + \mathrm{e}^{-2\pi^2 N^2 \xi \tau}) h_\epsilon^2(\tau). \tag{14}$$

Substituting (14) into (8) and using (7), we obtain our main result,

$$\sigma^2 = \frac{\alpha g_\epsilon(2\pi^2 N^2 \xi)}{N} \tag{15}$$

where

$$g_\epsilon(s) = 1 + \frac{\sum_{\tau=1}^{\infty} \mathrm{e}^{-s\tau} h_\epsilon^2(\tau)}{\sum_{\tau=1}^{\infty} h_\epsilon^2(\tau)}. \tag{16}$$

The function $g_\epsilon(s)$ interpolates between the limiting values for the time-reversal-invariant and non-time-reversal invariant cases [4]: $g_\epsilon(s)$ decreases from 2, when $s \ll \epsilon$, to 1, when $s \gg \epsilon$. For Lorentzian smoothing, i.e. $h_\epsilon(|\tau|) = \exp -(\epsilon|\tau|)$, the sums in (16) are easy to evaluate, and one obtains the explicit expression

$$g_\epsilon(s) = 1 + \frac{1 - \mathrm{e}^{-2\epsilon}}{1 - \mathrm{e}^{-(s+2\epsilon)}} \mathrm{e}^{-s}. \tag{17}$$

The smoothing width ϵ determines the scale over which the transition (15) occurs. Within the simple diagonal approximation employed here, its value cannot be precisely fixed, but it is constrained by the requirement that ϵ be smaller than the mean spacing $2\pi/N$. For consistency with the more general semiclassical method of [10], its value should be of the order of the mean level separation, i.e. $2\pi/N$ (it is under this assumption that the diagonal approximation can be justified). When comparing (15) to numerical results, we shall take $\epsilon = \pi/N$, i.e. half of the mean spacing.

For s small (for example, of order ϵ), expression (17) simplifies to

$$g_\epsilon(s) = 1 + \frac{1}{1 + s/2\epsilon}. \tag{18}$$

This expression is obtained by replacing the sums $\sum_{\tau=1}^{\infty}$ in (16) by integrals $\int_0^{\infty} \mathrm{d}T$, and therefore gives precisely the form of $g_\epsilon(s)$ appropriate for flows (as opposed to maps).

3. Perturbed cat maps

Cat maps, or hyperbolic automorphisms of the two-torus, are area-preserving maps of the torus of the form

$$\phi_M(z) = M \cdot z \bmod 1 \tag{19}$$

where $z = (q, p) \bmod 1$ and M is an integer matrix with unit determinant and trace greater than 2. Cat maps are amongst the simplest examples of hyperbolic systems. An exact

quantization procedure was found by Hannay and Berry [18]. (By exact, we mean that quantization of the iterated map, which is itself a cat map, gives the same result as iteration of the quantized map.) We will take

$$M = \begin{bmatrix} 2 & 1 \\ 3 & 2 \end{bmatrix} \tag{20}$$

for which the quantized map has a simple form. We note that ϕ_M is invariant under the time-reversal map $T(z) = (q, -p)$.

While the classical dynamics of the cat maps is generic, the quantum behaviour is not; degeneracies in the periodic orbit spectrum of number-theoretical origin lead to different spectral statistics than those of the circular ensembles of random matrix theory [19]. Basílio de Matos and Ozorio de Almeida [20] quantized nonlinear perturbations of the cat map (which, according to Anosov's theorem (see Arnold [21]), remain hyperbolic for small enough perturbations), and found their spectral statistics to be generic. As they demonstrated, particularly convenient perturbations from the point of view of quantization are near-identity shears in momentum and position. These are maps of the form

$$\sigma_p(q, p; \kappa_0) = (q, p - \kappa_0 F'(q)) \tag{21}$$

$$\sigma_q(q, p; \kappa) = (q - \kappa G'(p), p). \tag{22}$$

The parameters κ_0 and κ determine the perturbation strength. The semiclassical asymptotics of perturbed maps of this type was developed by Boasman and Keating [22].

We consider the family of maps

$$\phi = \sigma_q \circ \phi_M \circ \sigma_p \tag{23}$$

obtained by composing the cat map (19) with a fixed momentum shear σ_p and a family of position shears σ_q depending on κ. The momentum shear σ_p serves to break the number-theoretical degeneracies of the unperturbed cat map. However, because, like the cat map (19), σ_p is invariant under time reversal, the composition $\phi_M \circ \sigma_p$ is invariant under the anticanonical symmetries $T \circ \sigma_p$ and $\phi_M \circ T$. Thus, the spectral statistics of the singly sheared cat map are found to be COE [20]. The second shear in position destroys these anticanonical symmetries for $\kappa \neq 0$, and the spectral statistics of the doubly sheared cat map are typically found to be CUE.

The quantized maps are N-dimensional unitary matrices

$$U = (\mathcal{F} U_Q \mathcal{F}^\dagger) U_M U_P. \tag{24}$$

We give their explicit form in a position representation. The quantized cat map U_M is given by [18]

$$(U_M)_{jk} = (\mathrm{i}N)^{-1/2} \exp(2\pi \mathrm{i}(j^2 - jk + k^2)/N). \tag{25}$$

U_Q and U_P are diagonal matrices with elements $\exp(-2\pi \mathrm{i} N \kappa G(k/N))$ and $\exp(2\pi \mathrm{i} N \kappa_0 F(k/N))$ respectively. The matrix $\mathcal{F}_{jk} = \frac{1}{\sqrt{N}} \exp(2\pi \mathrm{i} jk/N)$ represents a finite-dimensional Fourier transform.

The shear functions F and G are taken to be

$$F(q) = \frac{1}{4\pi^2}\left(\sin 2\pi q - \frac{1}{2}\cos 4\pi q\right) \tag{26}$$

$$G(p) = \frac{1}{4\pi^2}\left(\cos 2\pi p - \frac{1}{2}\sin 4\pi p\right). \tag{27}$$

κ_0 is fixed to be 0.08. Given this value of κ_0, it can be shown, using the conditions of Anosov's theorem, that the perturbed map ϕ remains hyperbolic for κ ranging between

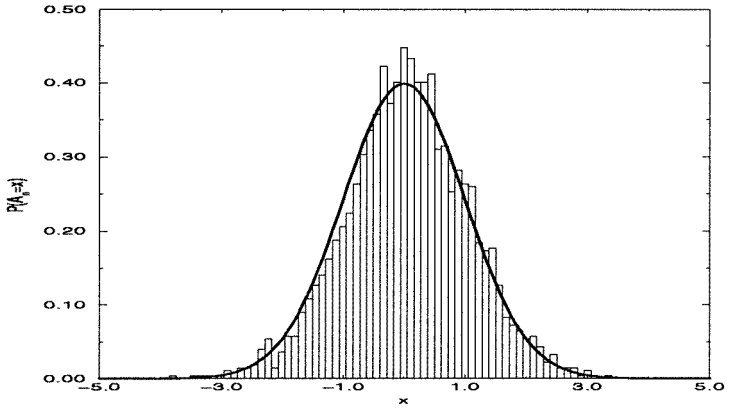

Figure 1. Scaled to their variance, the values of A_n for various values of N are shown, together with the normal distribution, in the limit of broken time reversal ($\kappa = 0.03$).

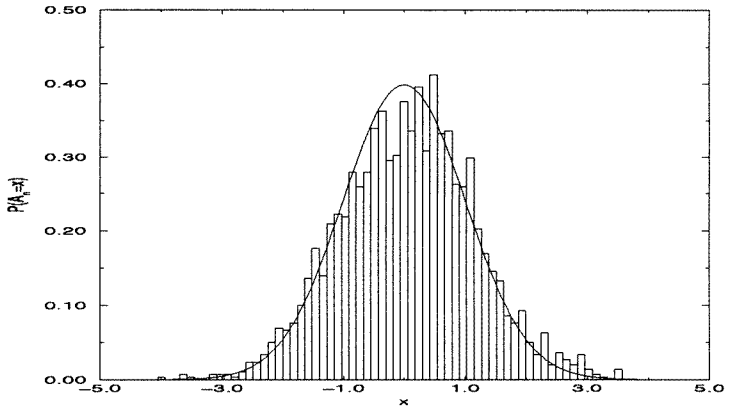

Figure 2. Scaled by the variance predicted by (15) and (17), the values of A_n for various values of N are shown, together with the normal distribution, in the transition regime ($\kappa = 0.003$).

between 0 and 0.03. For larger κ, the map dynamics becomes mixed, and the semiclassical structure is strongly affected by orbit bifurcations [23]. The theory developed in section 2 is only valid in the hyperbolic range.

4. Numerical results

We take $A = \cos 2\pi q$. In the position representation, A is represented by a diagonal matrix with elements $\cos(2\pi k/N)$. The classical observable $A_c(z) = \cos 2\pi q$ is invariant under the anticanonical symmetry $T \circ \sigma_p$, as is the classical map ϕ when $\kappa = 0$.

First let us consider the fully unitary case, which is achieved with $\kappa = 0.03$. In figure 1, we display a combined histogram of values of A_n for Hilbert spaces dimensions $N = 493, 495, 497, 499$ and 501. Each set of values is scaled to its variance $\frac{1}{N}\sum_{n=1}^{N} A_n^2$ to make the comparison with the superimposed Gaussian normal distribution.

In figure 2, we display the combined distribution of values of A_n for $\kappa = 0.003$, i.e. in the transition regime. The dimensions N are as above, and the values are scaled by

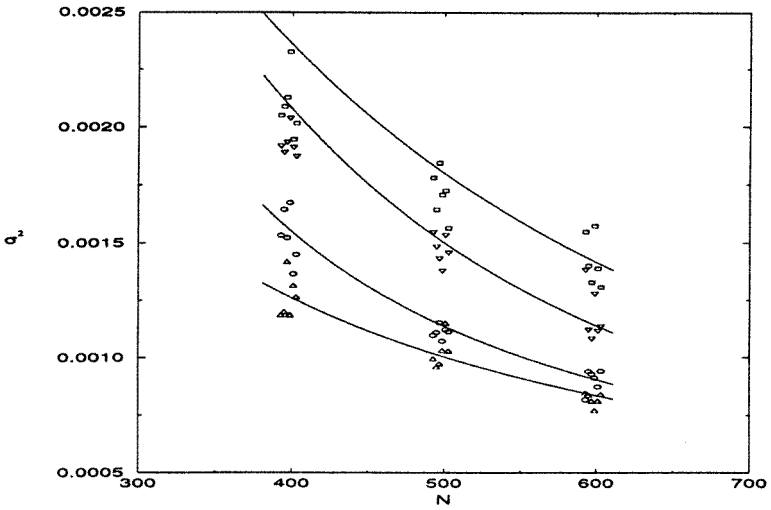

Figure 3. Variances for the operator $\hat{A} = \cos 2\pi q$, for values of N around 400, 500 and 600. κ assumes the following four values; 1×10^{-3}, squares; 2×10^{-3}, downward triangles; 5×10^{-3}, circles; and 3×10^{-2}, upward triangles. Superimposed are the semiclassical predictions (15) and (17) with $\epsilon = \pi/N$.

the variance predicted by the semiclassical formulae (15) and (17), with $\epsilon = \pi/N$. (It was checked that scaling with respect to the numerically computed variance, as in figure 1, makes no discernible difference.) ξ is estimated numerically from the classical dynamics, as discussed in the appendix. There are marked deviations in the computed distribution from Gaussian behaviour.

In figure 3, the numerically computed variances are compared with the semiclassical formulae (15) and (17) (ϵ and ξ are as above). The agreement is reasonably good, and improves with increasing N, as expected. It was confirmed that, provided ϵ is on the order of the mean spacing, the quality of the fit does not depend on its precise value.

There are two anomalies in the data. At $N = 501$ and $N = 593$, the computed variance for $\kappa = 0.005$ is actually less than that for $\kappa = 0.03$; i.e. the ordering of the upwards triangles and circles in figure 3 is reversed. To explain these anomalies, we have to recall the results of the linear cat map. First, the dimensions we worked with are all odd, with clusters around $N = 400$, 500 and 600. For instance, around 500, the values of N chosen were from 493 to 503 in steps of 2. We avoided even N's because their number-theoretical degeneracies are harder to break—they do not give generic random matrix statistics.

On the other hand, there is the high rigidity which occasionally occurs for a given N. This is another peculiarity owing to an unusually high quantum period function $n(N)$ for the propagator U_c [19]. For the problematic dimensions, we have $n(501) = 498$ and $n(593) = 594$.

In figure 4, we show the results for the total transition: COE to CUE. The semiclassical predictions do not depend on ϵ in this case.

5. Conclusions

We have developed a semiclassical theory for the transitional form of the variance of diagonal matrix elements of hyperbolic systems as time-reversal symmetry is gradually

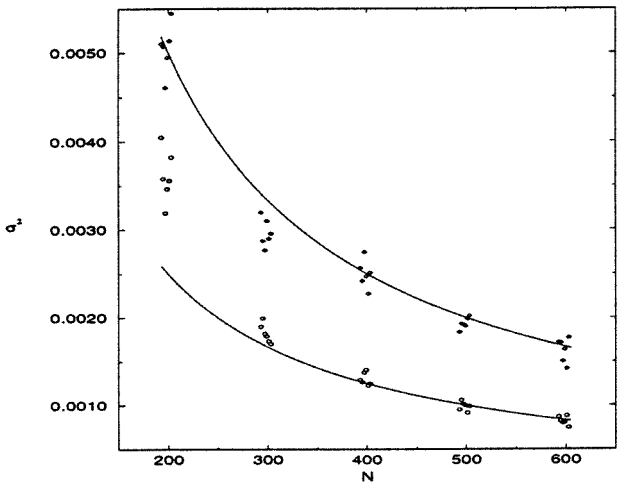

Figure 4. Variances for the operator A for $\kappa = 0$ (time-reversal symmetry intact), diamonds, and $\kappa = 0.03$ (time-reversal symmetry fully broken), circles. The lines are predictions of the semiclassical theory of [4], $g = 2$ and $g = 1$ in equation (15), respectively.

broken. The symmetry factor g in (1) is found to decrease from 2 to 1 as the symmetry-breaking parameter increases. There is good agreement with numerical calculations performed on a family of perturbed cat maps, specifically introduced to allow the effects of broken time-reversal symmetry to be studied.

The distribution of diagonal matrix elements in the transition regime shown in figure 2 exhibits interesting deviations from Gaussian behaviour, which we feel merit further investigation. It would also be interesting to compare our semiclassical approximation with exact results obtained from the nonlinear σ-model [24].

Acknowledgments

TOC thanks Conselho Nacional de Desenvolvimento Científico e Tecnológico, CNPq-Brazil, for a post-doctorate grant no 200.685/96-1.

Appendix. The variance of Δ_p

The relationship between the variance $\xi\tau_p$ of the action differences Δ_p and the perturbation constant κ can be deduced by a Taylor expansion of the actions. The first correction in the action in the perturbed case is of order κ^2, and therefore

$$\xi = c\kappa^2. \tag{28}$$

To determine the constant of proportionality numerically, the variance ξ was evaluated for a subset of periodic orbits of a given period, from $\tau = 3$ to $\tau = 15$. The results are shown in figure 5. Orbits invariant under time-reversal were discarded from the calculation. (As is easily verified for the unperturbed cat map (19), all period-two orbits are time-reversal invariant.)

With the exponential increase in the number of orbits with period, only a subset of the periodic orbits with $\tau \geqslant 8$ could be included. For a given period, this subset corresponded to orbits of the unperturbed cat map lying on a rational lattice with maximum denominator q.

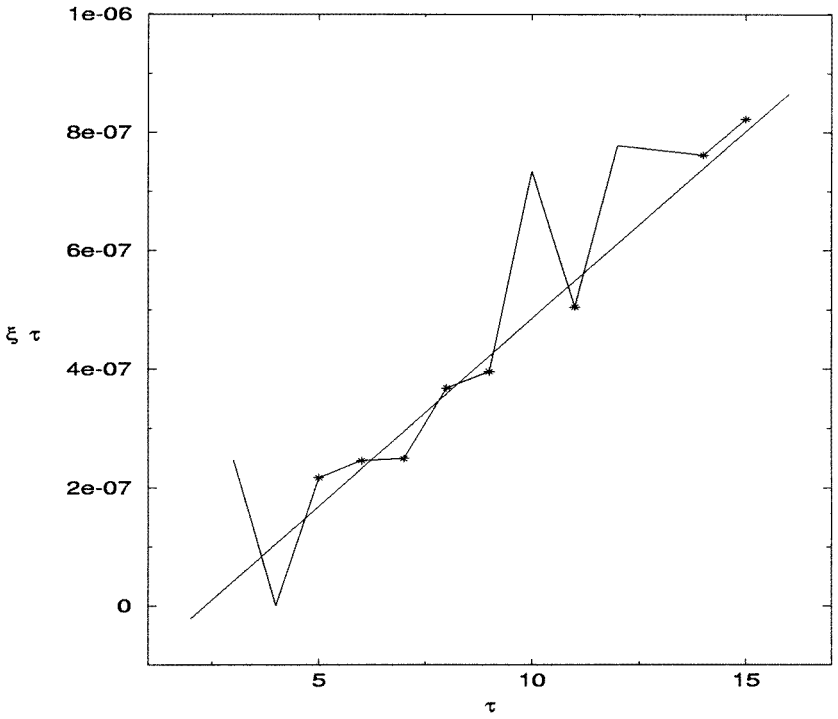

Figure 5. The variance of periodic orbit actions, $\xi\tau$, for $\kappa_p = 0.01$, together with a linear fit, for which $p(\tau) = 6.34 \times 10^{-8}\tau - 1.5 \times 10^{-7}$, and hence $c = 6.34 \times 10^{-4}$.

It so happens that all the orbits of period 13 are in the same rational lattice, with $q = 3691$. These orbits were not investigated, as the objectives of keeping all orbits on a rational sublattice and restricting computational efforts to a reasonable level were incompatible. Typically, for $\tau \geqslant 8$, hundreds of orbits were considered. Repetitions must be (and were) included in this calculation. κ was set to 0.01.

Although we have not used this approach, one could of course estimate the variance by computing action differences for nonperiodic orbits of given length τ, and averaging over initial conditions.

References

[1] Shnirelman A I 1974 *Usp. Mat. Nauk.* **29** 181–2
[2] Zelditch S 1987 *Duke Math. J.* **55** 919–41
[3] Colin de Verdiére Y 1985 *Commun. Math. Phys.* **102** 497–502
[4] Eckhardt B, Fishman S, Keating J, Agam O, Main J and Müller K 1995 *Phys. Rev.* E **52** 5893–903
[5] Bohigas O, Giannoni M J and Schmit C 1984 *Phys. Rev. Lett.* **52** 1–4
[6] Berry M V 1987 *Proc. R. Soc.* A **413** 183–98
[7] Bohigas O 1991 *Chaos et Physique Quantique* ed A Voros *et al* (Amsterdam: Elsevier) pp 89–199
[8] Hannay J H and Ozorio de Almeida A M 1984 *J. Phys. A: Math. Gen.* **17** 3429–40
[9] Berry M V 1995 *Proc. R. Soc.* A **400** 229–51
[10] Bogolmolny E B and Keating J P 1996 *Phys. Rev. Lett.* **77** 1472–5
[11] Andreev A V, Agam O, Simons B D and Altshuler B L 1996 *Phys. Rev. Lett.* **76** 3947–50
[12] Bohigas O, Giannoni M J, Ozorio de Almeida A M and Schmit C 1995 *Nonlinearity* **8** 203–21
[13] Shukla P and Pandey A 1997 *Nonlinearity* **10** 979–1006

[14] Leyvraz F, Schmit C and Seligman Th 1996 *J. Phys. A: Math. Gen.* **29** L575–80
[15] Keating J P and Robbins J M 1997 *J. Phys. A: Math. Gen.* **30** L177–81
[16] Wilkinson M 1987 *J. Phys. A: Math. Gen.* **20** 2415–23
[17] Berry M V and Robnik M 1986 *J. Phys. A: Math. Gen.* **19** 649–68
[18] Hannay J H and Berry M V 1980 *Physica* **1D** 267–90
[19] Keating J P 1991 *Nonlinearity* **4** 309–41
[20] de Matos M B and Ozorio de Almeida A M 1995 *Ann. Phys.* **237** 46–65
[21] Arnold V I *Geometrical Methods in the Theory of Ordinary Differential Equations*
[22] Boasman P A and Keating J P 1995 *Proc. R. Soc.* A **449** 629–53
[23] Berry M V, Keating J P and Prado S D 1998 *J. Phys. A: Math. Gen.* **31** 245–54
[24] Mehlig B Personal communication